http://dx.doi.org/10.15576/GLL/2021.4.55

GLL

Geomatics, Landmanagement and Landscape No. 4 • 2021, 55–73

SYNERGY OF PHOTOGRAMETRIC DATA OBTAINED BASED ON TERRESTRIAL PHOTOS AND UAV IMAGES

Izabela Piech, Wioletta Szyszka

Summary

Methods of short-range digital photogrammetry and unmanned aerial vehicle imagining increasingly find more extensive usage in various types of measurements. In recent years, modern photogrammetric technologies have found wide application in recreating 3D models of any objects. The resulting 3D models can be a source of information that may be used for measurement, inventorying and cataloguing, as well as for visualisation purposes.

New methods of acquiring spatial data have been developed, such as laser scanning, imaging using unmanned aerial vehicles or digital non-metric cameras. Synergy and the confluence of these data have expanded the existing measurement possibilities, finding application in 3D modelling, inventorying of monuments, or monument conservation. Photogrammetric methods are comparable to direct measurement methods in terms of their accuracy, as well as speed and cost. They have a number of advantages, including a shortened time required for taking a photo, which is greatly convenient when measuring moving objects. Other advantages of photogrammetric methods include the possibility of development and performing measurements in chamber conditions and the lack of restrictions pertaining to repeating the measurement when errors are found or a need arises to supplement them [Kurczyński and Preuss 2000]. One of the possibilities offered by photogrammetry is the ability to create 3D visualizations. The creation of a three-dimensional model facilitates presenting the inventoried object in a realistic, complete, and up-to-date manner. This paper presents an attempt to synergise data for modelling a three-dimensional architectural object based on photos obtained with the Nikon D7500 non-metric camera and with the DJI Mavic Air unmanned aerial vehicle.

Keywords

synergy • 3D models • non-metric cameras • unmanned aerial vehicles

1. Introduction

In recent years, modern photogrammetric technologies have found wide application in developing 3D models of buildings' façades. Three-dimensional models facilitate the representation of the inventoried object in a realistic, complete, and up-to-date manner. Such a virtual model offers a wide range of possibilities – among other things, it facilitates the use of various solutions for the expansion, remodelling, and most of all for the recon-

struction of the examined object [Boroń et al. 2007]. Orthophotomaps of building façades are usually developed using ground-based photogrammetry. Currently, it is no longer necessary to use massive photo-theodolites (that are metric cameras free from optical errors) in order to create photogrammetric studies, because modern computer software facilitates the application of digital cameras to this end. The use of photogrammetric techniques allows the use of metric or non-metric measuring cameras, and in recent years, ground-based laser scanners have been successfully deployed for the purpose. Among other authors [Kędzierski and Walczykowski 2008], [Zawieska 2008], [Kwoczyńska 2010, 2012] have discussed these issues. Unmanned aerial vehicles (UAVs) constitute another tool used to register architectural objects. Along with the development of UAV technology, unmanned aerial vehicles are also suitable for the development of orthophotomaps of the façades. This is extremely helpful for tall structures, making it possible to take pictures orthogonally to the building surface at any height. Unmanned aerial vehicles are becoming more and more popular in photogrammetry. Drones equipped with lightweight still or film cameras make it possible to scan, measure, and generate 3D models of the given area based on images recorded from the air. At the same time, they ensure greater flexibility and lower operating costs, and they are burdened with a lower risk than manned airplanes and helicopters [Olszewski and Ghaemi 2015]. The drone can be used for photogrammetric tests of built structures, which allow for the reconstruction of the shape, size and respective positioning of objects in the field on the basis of the photographs taken [Kostka 2014]. They are also used in order to perform measurements of the EGiB database of land and building records, which are very efficient even when compared to more advanced measurement methods. Photos obtained from the UAV range allow for a full assessment of the existing numerical resource of the cadastral records, not only in relation to the existing buildings, but above all, they make it possible to reliably demonstrate inaccuracies, deficiencies, or obvious errors in the definition of objects recorded in the cadastral database [Plichta et al. 2017].

In recent years, the idea of creating an independent, simple local geospatial data acquisition system based on unmanned aerial vehicles has emerged. The application of UAVs in spatial management has been tested, and the analysis of services provided by unmanned aerial vehicles in Poland was carried out. Based on the research conducted, it can be concluded that unmanned aerial vehicles constitute a helpful tool for urban planners, providing them with real-time data, enabling access to reliable information, implementing active monitoring, as well as streamlining and improving the spatial development process [Banaszek et al. 2017]. The objective of the present study was to create an orthophotomap using data obtained from a non-metric camera mounted on the DJI Mavic Air sports drone. This entailed a demonstration of the possibilities afforded by the unmanned aerial vehicle, when it comes to obtaining high-resolution material needed to develop orthophotomaps, and a comparing them to the results obtained from the measurement employing the Nikon D7500 non-metric digital camera. Additionally, the coordinates obtained as a result of tacheometric measurement, obtained from both measurement campaigns, were verified, and their quality and the generated errors were compared.

2. Research object

In this publication, the synergy of photogrammetric data obtained with a non-metric camera and the data from an unmanned aerial vehicle was achieved.

The subject of the study is the historic Roman Catholic Church of Our Lady of Perpetual Help, located in Rzepiska (Fig. 1).

Photo: W. Szyszka

Fig. 1. Church of Our Lady of Perpetual Help

3. Methodology

To achieve the intended goal, we have used: the Nikon D7500 non-metric camera with the Nikon DX VVR AF-P, Nikkor 18–55 mm f/3.5–5.6 AF-P VR DX lens, and the DJI Mavic Air unmanned aerial vehicle, the weight of which does not exceed 500 g. The CHC X900 GNSS receiver with a compatible controller was used to set up the geodetic control network. Photopoints were measured using the Topcon GTS 502E electronic total station. The UAV drone has a foldable structure and a three-axis gimbal with a camera that permits recording video material in 4K quality, and taking 12-megapixel photos. The maximum flight speed that the drone can achieve is 68.4 km per hour, while the maximum flight time is about 21 minutes in no wind conditions, with a constant speed of 25 km per hour.

The fieldwork included a drone flight, taking ground photos with the Nikon D7500 non-metric camera, and measuring photopoints in the form of 9 × 9 cm white-black targets located on the church's elevations (Fig. 2).

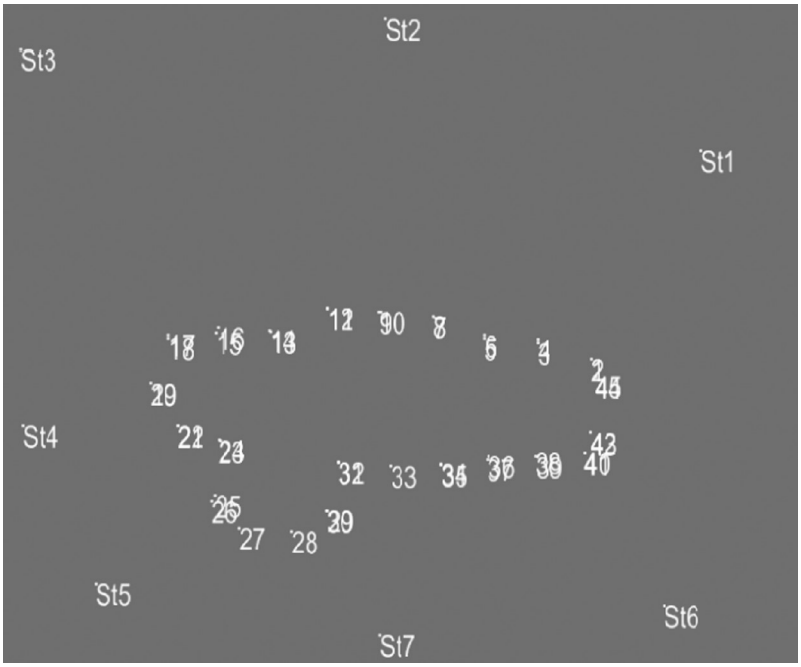

Source: Authors' own study

Fig. 2. Placement of measurement stations in relations to photopoints

Before the flight, a field visit was conducted in order to assess the feasibility of the flight and to select appropriate places for setting up the measurement network. Photopoints were signalled by targets that were placed evenly around the object in two rows. For the measurement control network, 7 stations marked as St1-St7 were designated. St1-St3 stations were stabilized with paint on an asphalt road, and St4-St7 stations were stabilized with pegs. The location of the measurement stations in relation to the photopoints located on the site is shown in Figure 3.

UAV images were taken around the object in two rows, while maintaining longitudinal coverage exceeding 60% and transverse coverage of 40% (Fig. 4). Having photographed the first (northern) façade, we have found that it was not possible to carry out the flight equidistant from the object, because there were trees on the flight path, particularly on the eastern side. Therefore, the flight coordinates were set manually due to the inability to determine uniform route for the entire object. During the flight, 135 photos were taken with the focal length set to the value of 24 mm.

Photo: W. Szyszka

Fig. 3. Sample photopoints used during the measurement

Photo: W. Szyszka

Fig. 4. Photographs taken at various heights

Having completed the flight with the unmanned aerial vehicle, photos were taken with a non-metric camera, maintaining the longitudinal and transverse coverage, just as during the photo shooting with the drone. The entire measurement was made on automatic settings with a focal length of 18 mm, obtaining 168 photos as a result. The last stage was the measurement of photopoints on the matrix in order to give the object an appropriate scale and georeference, as well as to determine the position of the camera and the orientation of the photos. There were 7 stations designated around the object so as to keep the vision for each photopoint from two measuring stations, and so that the angle between the two positions and the measured photopoint was equal to or greater than 90°. In order to determine the coordinates of the photopoints, the horizontal and vertical angles of each photopoint were measured from two measuring stations, and the distance to the mirror was measured for control. The calculation of

the coordinates was made based on angular forward intersection. The points where the distance to the mirror significantly differed from the distance obtained in the course of calculations were rejected from the study due to the probable measurement error. The height of the points was determined on the basis of the calculated distances and the measured vertical angles.

3.1. Elaboration of the acquired data

The chamber works were performed using the Agisoft PhotoScan software application. Two workspaces were set up, separately for photos taken with the drone, and those taken with the non-metric camera, and the same settings were introduced in both cases. For the purpose of georeferencing, the coordinates of the photo points were imported. Half of the photo points were selected for the study, so that the obtained coordinates could be checked on the remaining photopoints in the alignment of the photos.

After several photopoints have been marked (Fig. 5), on at least two photos, the images were aligned. The Agisoft software has an algorithm that allows the user to determine the position of the camera in relation to the object during the photo shooting.

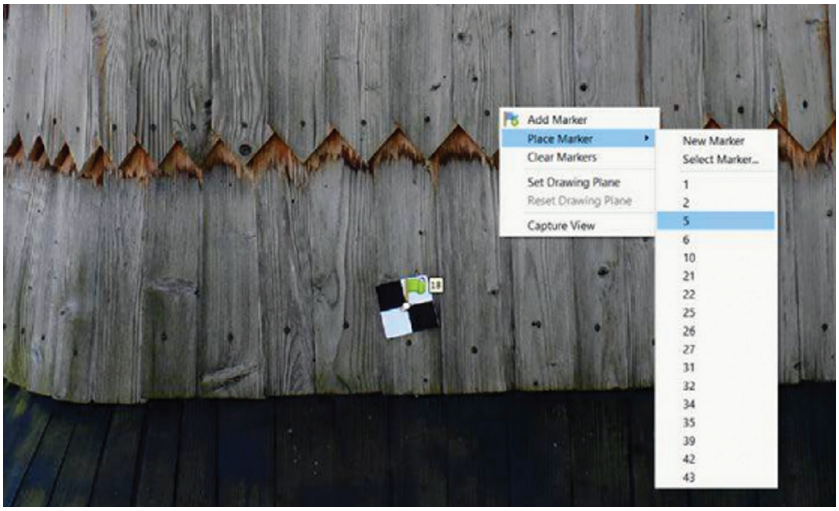

Source: Authors' own study

Fig. 5. Marking the photopoints

Having confirmed the correct location of all the photopoints involved in the alignment, a sparse point cloud obtained through alignment was generated and refreshed, which would not be used in the subsequent stages of model creation, but only represented the result of aligning the images. On the basis of the sparse point cloud, a region was created representing the volume for which further processing would be conducted.

At that stage, it was necessary to check if it had been generated correctly and, if necessary, to adjust the region for which a dense cloud of points and 3D models would then be developed.

The next step was to generate a dense point cloud based on photos taken with the Nikon D7500 non-metric camera. Since the cloud is burdened with numerous instances of noise, such as mapped tree branches and possible distortions, it has been subjected to cleaning. Figure 6 shows a cleared dense point cloud.

Source: Authors' own study

Fig. 6. Dense point cloud (Nikon D7500 non-metric camera)

Then, a 3D model was created, represented by a triangle mesh, interpolated on points from a dense point cloud (Fig. 7).

On the church façade, parallel to the projection plane, 2 points were marked, which designated the main axis of the mapping projection. In order to avoid the orthophotomap being warped in relation to the coordinates' system, these markers were placed at the same height. Then, the size of the field pixel was determined, which for the orthophotomap generated by means of photos taken with the Nikon D7500 non-metric camera was set at 0.72 mm, while for the drone, it was set at 1.5 mm.

Figure 8 shows the generated orthophotomap of the southern elevation.

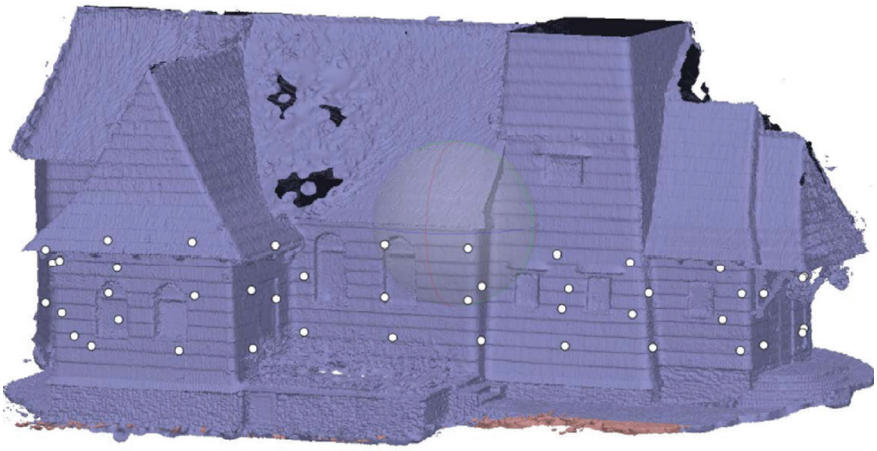

Source: Authors' own study

Fig. 7. 3D model represented by the skeletal mesh

Source: Authors' own study

Fig. 8. Orthophotomap of the southern elevation (Nikon D7500 SLR camera)

4. Research results

In order to analyse the accuracy of the created models, the coordinates of the photo-points were read from 3D models generated on the basis of data obtained from the Nikon D7500 non-metric camera, and from the DJI Mavic Air drone. The read coordinates were compared with the coordinates obtained as a result of the tacheometric measurement. Table 1 contains the absolute values of the differences between the coordinates calculated from the tacheometric measurement, and those read from individual 3D models, along with the minimum, maximum, and mean values.

Table 1. Differences of coordinates – between the coordinates obtained from the measurements, and those obtained from the models generated using the UAV and the camera

No.	Non-metric camera			Unmanned aerial vehicle		
	m_x	m_y	m_z	m_x	m_y	m_z
1	0.004	0.010	0.006	0.124	0.028	0.051
2	0.009	0.009	0.002	0.120	0.046	0.038
3	0.021	0.014	0.002	0.012	0.015	0.007
4	0.004	0.003	0.014	0.006	0.010	0.004
5	0.013	0.012	0.006	0.017	0.005	0.010
6	0.008	0.000	0.002	0.000	0.001	0.005
7	0.014	0.014	0.006	0.029	0.006	0.014
8	0.018	0.013	0.011	0.032	0.007	0.009
10	0.008	0.003	0.005	0.009	0.009	0.001
11	0.008	0.005	0.005	0.009	0.006	0.009
12	0.006	0.013	0.001	0.013	0.005	0.002
13	0.005	0.012	0.005	0.008	0.000	0.007
14	0.016	0.006	0.006	0.001	0.018	0.000
16	0.005	0.004	0.002	0.029	0.025	0.014
17	0.035	0.005	0.011	0.004	0.001	0.005
18	0.019	0.007	0.015	0.008	0.002	0.013
19	0.003	0.012	0.024	0.011	0.040	0.039
20	0.002	0.015	0.015	0.022	0.050	0.025
21	0.009	0.000	0.019			
22	0.006	0.004	0.019			
23	0.005	0.002	0.023	0.116	0.037	0.028
24	0.005	0.000	0.018	0.108	0.008	0.019
26	0.003	0.006	0.007	0.016	0.016	0.007
27	0.047	0.017	0.015	0.015	0.038	0.031
28	0.046	0.017	0.024	0.018	0.031	0.010
29	0.008	0.070	0.005	0.066	0.084	0.015
30	0.007	0.004	0.017	0.081	0.028	0.018

Table 1. cont.

No.	Non-metric camera			Unmanned aerial vehicle		
	m_x	m_y	m_z	m_x	m_y	m_z
31	0.018	0.016	0.009	0.112	0.016	0.019
32	0.005	0.015	0.008	0.079	0.015	0.005
33	0.001	0.001	0.005	0.100	0.013	0.004
34	0.008	0.007	0.004	0.108	0.022	0.022
35	0.013	0.012	0.001	0.087	0.038	0.009
36	0.000	0.001	0.005	0.123	0.026	0.025
37	0.007	0.011	0.047	0.116	0.018	0.053
39	0.003	0.002	0.003	0.097	0.055	0.007
40	0.009	0.005	0.008	0.107	0.060	0.036
41	0.014	0.014	0.007	0.092	0.051	0.016
42	0.014	0.009	0.003	0.129	0.042	0.032
43	0.005	0.006	0.010	0.113	0.040	0.026
44	0.007	0.002	0.013	0.120	0.049	0.063
45	0.020	0.004	0.012	0.141	0.033	0.050
Max	**0.047**	**0.070**	**0.047**	**0.141**	**0.084**	**0.063**
Min	**0.000**	**0.000**	**0.000**	**0.000**	**0.000**	**0.000**
Mean	**0.011**	**0.009**	**0.010**	**0.062**	**0.026**	**0.019**

By analysing the differences in the obtained coordinates, it becomes apparent that the model obtained by processing photos taken with a non-metric camera fits better into the target coordinate system, and the maximum error values are much smaller than in the case of the model created with images taken with the drone. However, it is also apparent that the high error values from the drone measurement are more local in nature. The error values on points from 3 through 28 for both models are comparable with each other, which can also be seen in the significant decrease in the mean error value in relation to the maximum values presented in Table 1. Having analysed the coordinates themselves, we can conclude that the software application struggled with mapping some parts of the object (no reading of coordinates for points 21 and 22 from the model created with photos taken with a drone). This loss is caused by a fragment of the west façade wall that is not mapped on the model due to the presence of shaded areas. Figure 9 shows a view of the southwest façade mapped with photos taken with a drone, with Figure 10 showing the same façade mapped with photos taken with a Nikon non-metric camera.

Source: Authors' own study

Fig. 9. Model of the south-western wall obtained using the UAV

Source: Authors' own study

Fig. 10. Model of the south-western wall obtained using the Nikon non-metric camera

In order to verify the correctness of the generated models for individual walls of the church, differential models were made based on the model created from the data obtained from the drone, and the model created based on the data from the non-metric

camera. Having analysed the coordinate differences, we note that the models faithfully reflect the examined object. Figures 11–20 show the differential elevation models created in Cloud Compare with a scale, the colour intensity of which symbolizes the distance between the models at all its points.

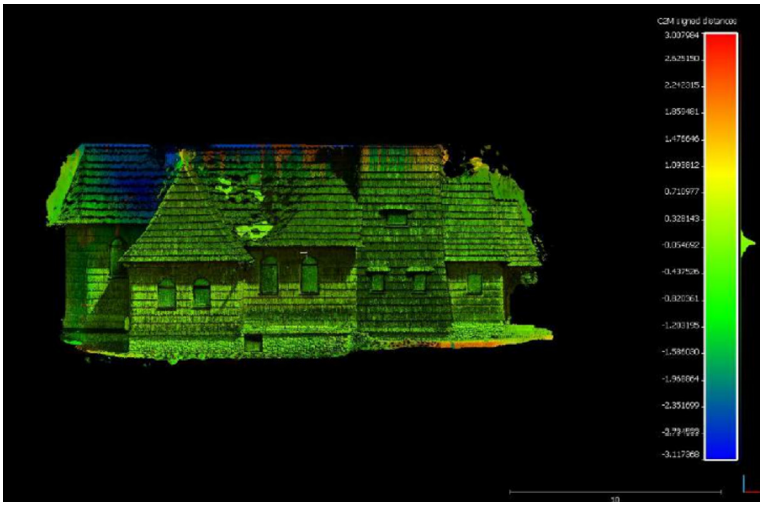

Source: Authors' own study

Fig. 11. Differential model of the southern elevation (the camera versus UAV)

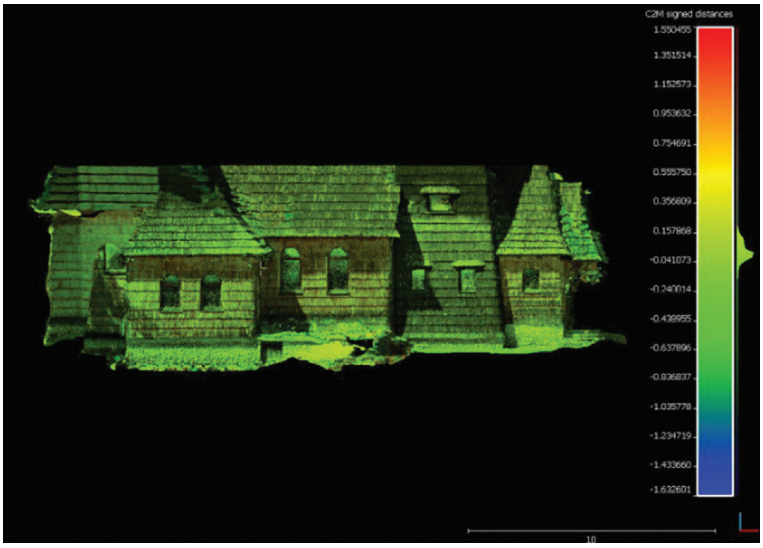

Source: Authors' own study

Fig. 12. Differential model of the southern elevation (UAV versus the camera)

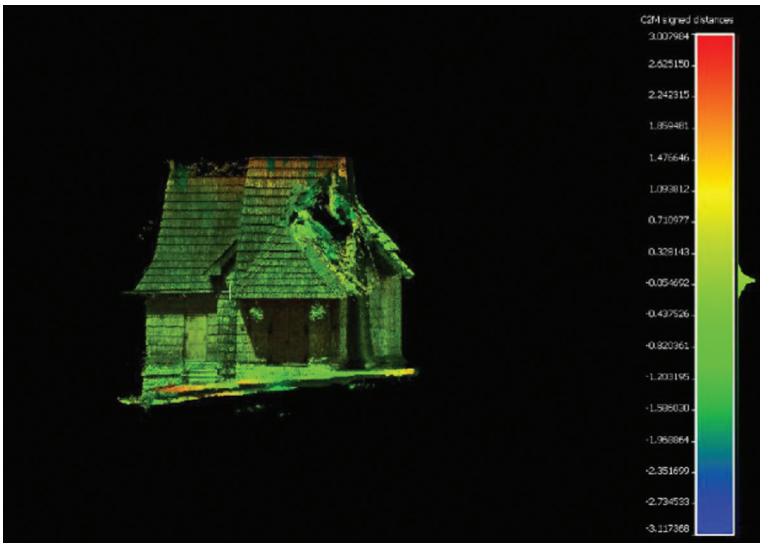

Source: Authors' own study

Fig. 13. Differential model of the eastern elevation (the camera versus UAV)

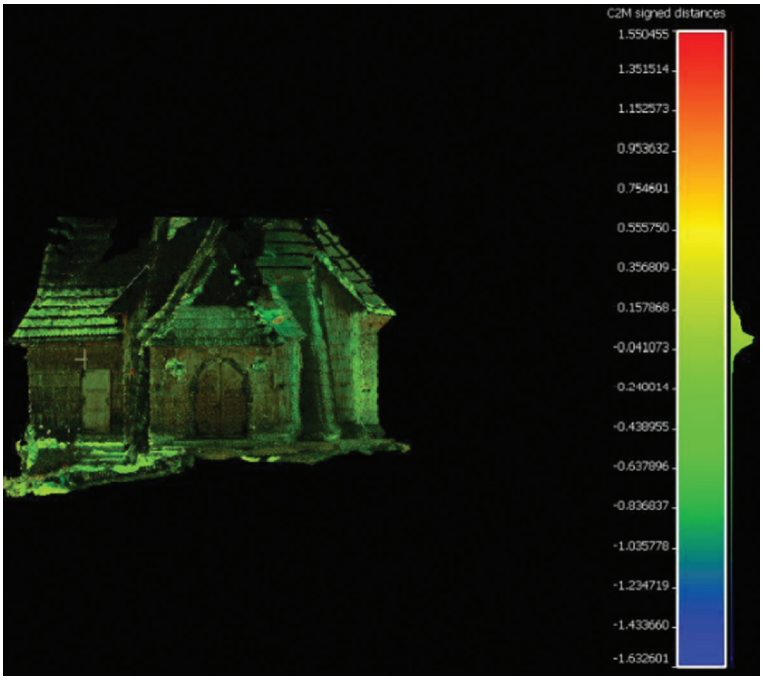

Source: Authors' own study

Fig. 14. Differential model of the eastern elevation (UAV versus the camera)

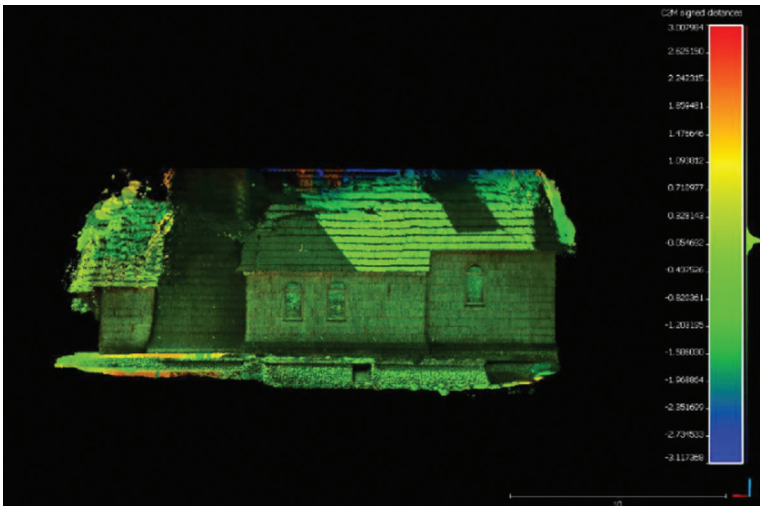

Source: Authors' own study

Fig. 15. Differential model of the northern elevation (the camera versus UAV)

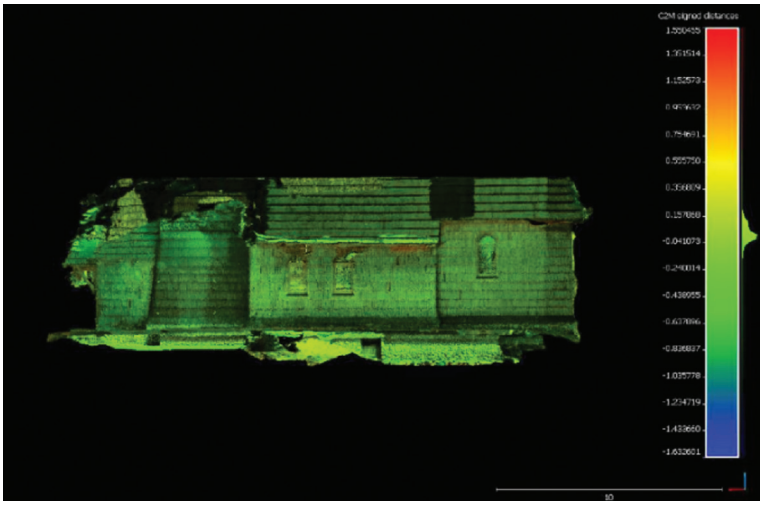

Source: Authors' own study

Fig. 16. Differential model of the northern elevation (UAV versus the camera)

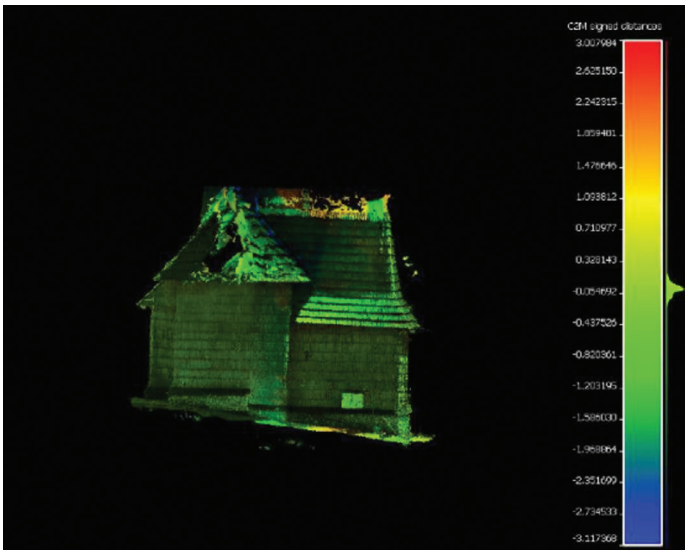

Source: Authors' own study

Fig. 17. Differential model of the eastern elevation (the camera versus UAV)

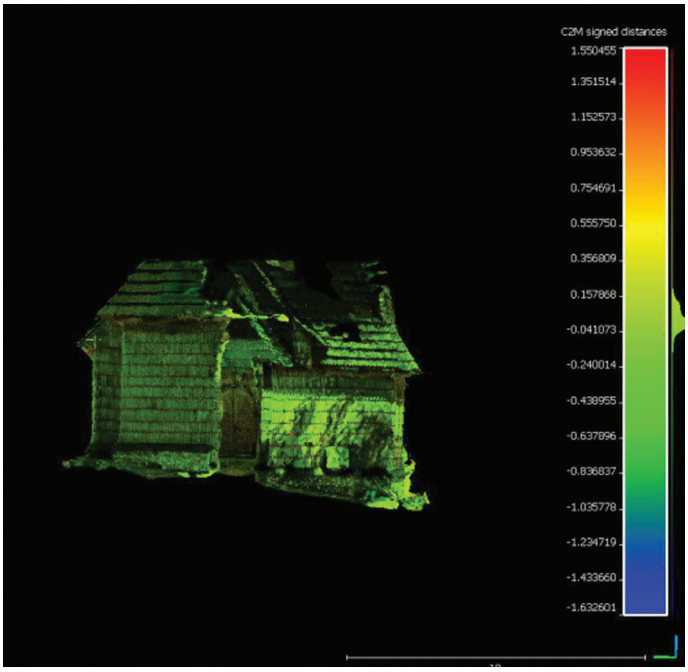

Source: Authors' own study

Fig. 18. Differential model of the eastern elevation (UAV versus the camera)

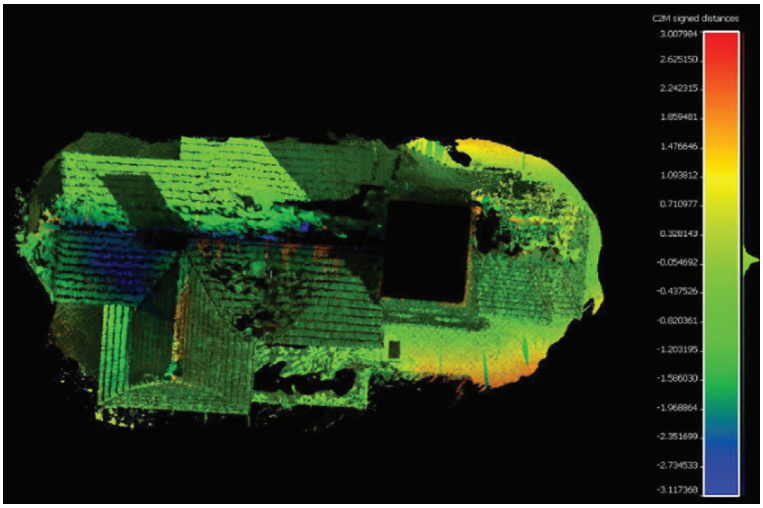

Source: Authors' own study

Fig. 19. Differential model of the top view (the camera versus UAV)

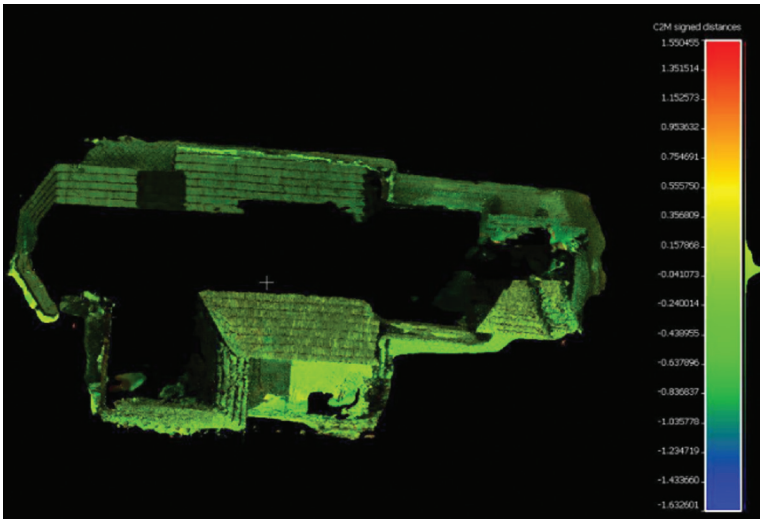

Source: Authors' own study

Fig. 20. Differential model of the top view (UAV versus the camera)

Note that in the presented differential models the dominant colour is green, which represents the difference in distances between the models that is close to zero. As the colour approaches blue or red, this signifies increased distance in one direction or the other. Such deviations can be observed in a small number of fragments, usually characterized by various types of distortions. The mere fact of distortion in these areas in all likelihood signifies an error in generating the model, which is most often caused by incorrectly taken photos. When assessing the orthophotomaps, it was found that the northern, southern and then eastern walls are the best exposed. Thanks to the lack of barriers during the flight, and the fact that the church walls are well lit, they are not burdened with visual distortions, and the images are suitably sharp and detailed. The worst quality is found in the western wall, especially in the south-western part, due to the fact that some spots are poorly accessible for a flight using unmanned aerial vehicles. In the shaded areas, there are distortions as well as gaps in the model. Despite attempts to exclude the worst quality photos from the mosaic process, it was not possible to achieve a satisfying result for the orthophotomap of the western façade. Images taken with a non-metric camera have a size of 5568 × 3712 and a resolution of 300 dpi, while pictures taken with a drone have a size of 960 × 720 pixels and a resolution of 96 dpi. The difference is very significant, and it also translates into the quality of the orthophotomaps. Differences can also be noticed when generating an orthophotomosaic, where in the case of the drone the value of the field pixel is 1.5 mm, while for a non-metric camera this value is more than two times smaller, and amounts to 0.72 mm. Figure 21 shows the same approximate fragment of a correctly mapped surface, enabling a visual assessment of the quality of representation.

Source: Authors' own study

Fig. 21. Comparison of the mapping quality

5. Conclusions

The study attempts to synergize photogrammetric data, obtained from the application of various tools. When analysing the possibilities of using two specific techniques to generate a 3D model, attention was paid to the problems encountered during their development and elaboration. The possibilities were presented, followed by a comparison between the results of the photogrammetric study made with the use of a sports drone (unmanned aerial vehicle) and with the tool commonly used for this purpose (a non-metric camera). Having conducted the analysis, the following conclusions were drawn: firstly, attention should be paid to the selection of the instrument's position, and secondly, the correct execution of the flight is of utmost importance, because the success of the entire mission depends on it. During the design process, parameters are determined such as the points of the vehicle's turning, the points of the shutter opening, as well as the flight speed and altitude. Before the plan was implemented, a field visit was essential in order to verify the existence of tall objects, such as trees, that might obscure some walls of the building. It was found that the sports drone is a good alternative to the more expensive and professional counterparts. Despite the lower image resolution that it offers, the photos taken with the non-metric sports camera do not differ significantly in quality and are free from optical errors that might cause colour distortions of the representations. The models obtained with both methods can work together, but each of the methods has its drawbacks that could be cross-eliminated.

Funded by a subsidy from the Ministry of Education and Science for the University of Agriculture in Krakow for 2021.

References

Banaszek A., Cellmer A., Banaszek S., Żarnowski A. 2017. Zastosowanie nowych technologii pozyskiwania danych geoprzestrzennych w gospodarce przestrzennej. Prace Naukowe Uniwersytetu Ekonomicznego we Wrocławiu, 281–291.

Boroń A., Rzonca A., Wróbel A. 2007. Metody fotogrametrii cyfrowej i skanowania laserowego w inwentaryzacji zabytków. Rocznik Geomatyki, 2–4.

Kędzierski M., Walczykowski P., Fryśkowska A. 2008. Wybrane aspekty opracowania dokumentacji architektonicznej obiektów zabytkowych. Archiwum Fotogrametrii, Kartografii i Teledetekcji, 18a, 221–230.

Kostka S. 2014. Fotogrametria – stara technika w nowym wydaniu. Wydawnictwo Jaskinie, 3 (76), 14–16.

Kurczyński Z., Preuss R. 2000. Podstawy fotogrametrii. Oficyna Wydawnicza Politechniki Warszawskiej, Warszawa, 6–7.

Kwoczyńska B. 2010. Opracowanie obiektów architektonicznych z wykorzystaniem metod stosowanych w fotogrametrii cyfrowej. Infrastruktura i Ekologia Terenów Wiejskich. PAN Oddział w Krakowie, 3, 65–74.

Kwoczyńska B. 2012. Inwentaryzacja i wizualizacja obiektów architektonicznych wykonana na podstawie zdjęć metrycznych i niemetrycznych. Infrastruktura i Ekologia Terenów Wiejskich, PAN Oddział Kraków, 1/II, 53–66.

Olszewski H., Ghaemi M.H. 2015. Drony. Nowy sposób na rejestrację danych fotogrametrycznych. Nowa Geodezja w Praktyce, 5–16.

Plichta A., Wyczałek M., Wyczałek I. 2017. Opracowanie części graficznej ewidencji gruntów i budynków w oparciu o zdjęcia lotnicze z pokładu UAV. Zeszyty Naukowe, 165, 36–48.

Zawieska D. 2008. Rekonstrukcja 3D obiektów bliskiego zasięgu na podstawie zdjęć archiwalnych. Archiwum Fotogrametrii, Kartografii i Teledetekcji, 18b, 717–726.

Dr inż. Izabela Piech
University of Agriculture in Krakow
Department of Land Surveying, Cadastre and Photogrammetry
30-198 Kraków, ul. Balicka 253a
Correspondence address:
31-120 Kraków, al. Mickiewicza 21
e-mail: rmpiech@cyf-kr.edu.pl
ORCID: 0000-0002-6710-4387

Mgr Wioletta Szyszka
University of Agriculture in Krakow
Department of Land Surveying, Cadastre and Photogrammetry
30-198 Kraków, ul. Balicka 253a
Correspondence address:
31-120 Kraków, al. Mickiewicza 21
e-mail: wiolettahaj@gmail.com